Published in final edited form as:
Arch Oral Biol. 2007 September ; 52(9): 814–821.

Elevated TGF-β2 signaling in dentin results in sex related enamel defects

Kuniko Saeki[a], **Joan F Hilton**[b], **Tamara Alliston**[c], **Stefan Habelitz**[a], **Sally J Marshall**[a], **Grayson W Marshall**[a], and **Pamela DenBesten**[d,*]

a*Preventive and Restorative Dental Sciences, University of California, San Francisco, Box 0758, 707 Parnassus Ave, San Francisco, CA 94143-0758, USA*

b*Epidemiology & Biostatistics, University of California, San Francisco, Box 0560, 185 Berry Street 5700, San Francisco, CA. 94107-1762, USA*

c*Department of Orthopaedic Surgery, University of California, San Francisco, Box 0514, 533 Parnassus Ave, San Francisco, CA94143-0514, USA*

d*Department of Orofacial Sciences, University of California, San Francisco, Box 0422, 707 Parnassus Ave, San Francisco, CA 94143-0422, USA*

Abstract

Initiation of enamel formation requires reciprocal signaling between epithelially and mesenchymally derived cells.

Objective—In this study, we used a transgenic mouse model which drives overexpression of an activated form of TGF-β2 under control of the osteocalcin promoter, to investigate the role of TGF-β2 in the dental mesenchyme, on enamel formation.

Design—Dentin and enamel were imaged by scanning electron microscopy (SEM) and atomic force microscopy (AFM). Dentin mechanical properties were characterized for hardness and elasticity, following nanoindentation with a modified AFM. Pores found in enamel were quantified and compared using image analysis software (Scion Image™).

Results—The elastic modulus of dentin was significantly reduced in the male TGF-β2 overexpressor mice as compared to male wildtype mice, with no significant differences between female mice. Similarly, there were significantly more pores in the male transgenic mice as compared to male wildtype mice, with no significant differences between female mice. *In-situ* hybridization of the continuously erupting incisor confirmed that osteocalcin expression was limited to the odontoblast cell layer at all stages of tooth formation.

Conclusion—TGF-β2 overexpression in the dentin matrix, results in sex-linked differences in dentin and enamel formation.

Keywords

Dentin; TGF-β2; enamel; osteocalcin; AFM; sex-linked

* Corresponding Author University of California, San Francisco, California, USA, Box, 0422, San Francisco, CA, USA 94143-0422, Tel: 415-502-7828, Fax: 415-476-1499, E-mail: pamela.denbesten@ucsf.edu

Introduction

Teeth form in a highly ordered process that includes reciprocal signaling between the epithelium and mesenchyme (1,2). Differentiation of odontoblasts from the dental mesenchyme requires signals from the oral epithelium. Subsequent to the initiation of dentin formation, ameloblasts differentiate from the oral epithelium to begin enamel formation.

TGF-β family ligands are known to regulate a number of epithelial and mesenchymal tissue interactions. For example, loss of TGF-β signaling in mice and humans has been implicated in cleft palate defects resulting from impaired epithelial/mesenchymal interactions (3-5). The expression pattern of TGF-β family ligands, receptors, and downstream Smad effectors in the developing tooth and in odontogenic tumors suggests that these growth factors are also important for the epithelial/mesenchymal interactions required for tooth development (6-8) (for reviews see (9-11)

In vitro studies have shown that pulp cells express several members of the TGF-β ligand family including TGF-β1, BMP-2, and BMP- 4 (12). Liu *et al.* showed that when pulp cells grown *in vitro* differentiate into an odontoblast phenotype, TGF-β3, Smad3, and Smad8 are strongly upregulated (>10X), as well as TGF-β2, and TGF-β receptor I (> 3 X)(13). As pulp cells express both ligands and receptors for the TGF-β family, these growth factors can regulate cell proliferation and differentiation in autocrine and paracrine manners (14). Clearly, the TGF-β signaling pathway is intact and important in odontoblast differentiation and tooth development. However, the mechanisms by which TGF-β acts to control dentin and enamel formation remain unclear. For example, TGF-β1 has been shown to stimulate pulp cell proliferation but inhibit odontoblast differentiation, whereas, Huojia and co-workers showed that TGF-β3 enhanced terminal odontoblast differentiation and promoted the formation of ectopic dentin (15). The relevance of these in vitro studies to tooth formation is difficult to assess in view of the complicated epithelial mesenchymal interactions of tooth development in vitro.

Therefore, in this study we investigated the role of TGF-β in tooth formation *in vivo* by using transgenic mice that express the active form of TGF-β2 under control of a 1.8-kb fragment of the rat osteocalcin promoter, made by Erlebacher and Derynck (16). The D4 line of these transgenic mice express 16-fold elevated levels of TGF-β2 in cells that express osteocalcin, including osteoblasts, odontoblasts and cementoblasts. Because osteocalcin expression has only been reported in the dental mesenchyme, but not in the enamel epithelium or differentiated ameloblasts (17,18), this transgenic mouse model is useful in understanding the effects of TGF-β signaling by the dental mesenchyme on enamel. The aim of this study was to determine whether changes in TGF-β2 expression by cells of the dental mesenchyme would also affect enamel formation.

Materials and Methods

SEM and AFM analysis of D4 and WT teeth

D4 mice (16), containing the plasmid pOc-β2C2S2, which expresses 16-fold elevated levels of active TGF–β2 under control of the osteocalcin promoter, were used for these studies. Eight week old male (n=3) and female (n=4) D4 mice, and their age and sex matched controls (male: n=3 and female n=4) were killed by CO_2 inhalation, followed by cervical dislocation according to UCSF approved animal care protocols. The lower mandible was removed. Following dissection of excess soft tissue, isolated mandibles were placed into Hanks' balanced salt solution prior to embedding in epoxy resin (Stycast, Emerson & Cuming, MA). The mouse mandibles were polished using SiO_2 abrasive paper to the center of the pulp chamber to provide sagittal sections of the first molar crown. The samples were further polished with a series of abrasive papers down to 1200 grit (American National Standards Institute, ANSI #1200) and

then with water based diamond suspensions down to 0.25 μm particle size (Buehler, Ltd., Lake Bluff, IL). The sections were cleaned ultrasonically in deionized water for 10 seconds and imaged by light microscopy and scanning electron microscopy (SEM) (ISI ABT, SX-40A, Topcon Instruments, Pleasanton, CA) using back scattered imaging.

Mechanical properties of the specimens were studied immediately after final surface preparation using atomic force microscopy (AFM) based nanoindenation, (Nanoscope III, Digital Instruments, Santa Barbara, CA) with the standard head replaced by a Triboscope nanoindenter system (Hysitron Inc., Minneapolis, MN), as described elsewhere (19,20). Nanoindentations were made in a liquid cell containing distilled and filtered water ("wet" condition). A Berkovich diamond indenter with a tip radius of about 20 nm or Berkovich indenter, radius around 100nm was used for indentation and imaging. Fused silica was used for calibration of the machine compliance, the elastic modulus, and to define the tip area function for indentation depths over a range of 50 to 200 nm. Indentation loads of 750 μN on dentin resulted in indentation depths 150-200nm. A linear series of indentations, spaced approximately 10μm apart, were made in each specimen. AFM imaging ensured positioning of the indenter on the intertubular dentin while avoiding tubules and the peritubular region. The indentation load-displacement data were analyzed to determine the elastic modulus, according to the method of Oliver and Pharr (21,22).

Analysis of pores in the enamel matrix

Backscattered imaging of the enamel overlying the dentin-enamel junction (DEJ) showed the presence of pores that were further imaged by conventional atomic force microscopy (AFM) (Nanoscope III, Digital Instruments, Santa Barbara, CA). For each first molar, 8 positions, 2 in the cervical region, 3 in the occlusal region, and 3 in the proximal region, were selected. At each position, AFM topographic images 50μm × 20μm of the enamel adjacent to the DEJ and mid-enamel (100μm from the DEJ) were obtained (Fig. 1A).

Pores noted in AFM topographic images were analyzed using image analysis software (Scion Image™). An example of the AFM images and their processing is shown in Figure 2. Within each 1000 μm^2 field, the number of pores was counted and their individual sizes were recorded. Individual pore sizes were summed to estimate the area of the field occupied by pores. The image analysis technique for identifying pores depends on a subjective identification of the periphery of a pore. Wider peripheries result in fewer distinct pores, since some pores then merge together, but a larger cumulative area. Consequently, this measurement error accumulates with pore count and pore area. For a given field, we controlled this effect by repeatedly defining the periphery, on the basis of a relatively large "index" pore within the field, and then selecting typical data (pore count, cumulative area) for analysis.

Statistical Analysis

To model random effects for pore area and pore number, we accounted for clustering of outcomes within mice, since there was sufficient data to support this approach. On the natural scale, both outcome variables, pore area and pore count, were right skewed before log transformation but were approximately normally distributed afterwards, judging from QQ plots and Kolmogorov-Smirnov tests. When the transformed data were stratified by tooth, no extreme outlier was identified for either outcome variable.

We used mixed effects models to examine the dependence of each outcome variable on the fixed effects of mouse type (D4 or WT), sex, tissue type (enamel at the DEJ or mid-enamel), and field position (cervical, occlusal, or proximal). For mouse-type, sex, and tissue-type, all two-way interaction terms and the 3-way effect were included in the models of both outcomes. In addition, the models were adjusted for pairing of tissue types within the 8 locations along

the DEJ (see Figure 1; 5 locations shown) as well as for nesting of tissue types and locations within mice. Analyses were performed on the log scale, and means and confidence intervals were transformed to the natural scale for reporting. Findings are presented both overall and by field position (cervical, occlusal, and proximal).

In situ hybridization

Mandibles from 2 WT and 2 D4 mice were fixed overnight in 4% paraformaldehyde, demineralized in 10% EDTA, embedded in paraffin, and sectioned in RNAse free conditions. A ^{35}S-labeled cRNA osteocalcin antisense probe was generated following linearization of the corresponding plasmid with BamHI and *in vitro* transcription using T3 polymerase as described by Ferguson and co-workers (23). As a negative control, a ^{35}S-labeled cRNA histone deacetylase 5 (HDAC5) sense probe was generated by linearization of pRK5-HDAC5 with XbaI and transcription using Sp6 polymerase as described,(24). Sections were counterstained with 4', 6-diamidino-2-phenyindole (DAPI) to visualize nuclei. Dark-field illumination was used to reveal *in situ* labeling, which was then colorized using Adobe Photoshop to evaluate localization of osteocalcin mRNA expression.

Results

Examination of the dentin under light microscopy and SEM revealed no obvious structural difference in the dentin of WT as compared to either the male or female D4 mice (data not shown). However, backscattered SEM showed pores in enamel at the DEJ and into the mid enamel region (Fig.1).

Dentin Mechanical Properties

Dentin elastic modulus was found to be significantly lower in male D4 mice than in other groups ($P = 0.0009$) (Table 1). For hardness measurements, variation by group was less dramatic ($P = 0.17$), but this outcome was again lowest in male D4 mice (Table 1).

Porosity in enamel

To gain a better understanding of the structure near the DEJ, we utilized AFM which visualizes the DEJ region with less sample distortion. Figure 3 shows typical AFM images of the enamel pores. AFM was used to quantify the porosity in enamel near the DEJ. In 1000 μm^2 fields of enamel, pores occupied an average of 1.7% of the surface area (range, 0.03% to 20.3%). Pore areas were greatest in D4 male mice (Figure 4). Near the DEJ, pores occupied 6.4% of the 1000 μm^2 image in D4 male mice, compared with 2.6% in D4 female mice, 2.3% in WT male mice and 1.8% in WT female mice (Figure 4a).

The relationship between mouse type and sex seen in enamel near the DEJ also was observed in the mid-enamel; however, the pore areas in the mid-enamel region occupied significantly less area by a factor of 3.35 (95% confidence interval (CI), 2.52 to 4.44; $P < 0.001$) In addition, pore count was consistently higher near the DEJ than in mid-enamel (DEJ:mid-enamel ratio, 1.81; $P = 0.004$). Among D4 mice, pore area was significantly greater in males than females by a factor of 2.58 (95 % CI, 1.48 to 4.51; $P = 0.002$), whereas among WT mice pore area hardly varied by sex (male:female ratio, 1.23 (0.70 to 2.15; $P = 0.45$)). Further, among male mice, pore area was larger in D4 than WT mice by a factor of 3.13 (1.57 to 6.26; $P = 0.004$) but among female mice, the D4:WT ratio was only 1.48 (0.81 to 2.69; $P = 0.18$). Pore size was larger in male D4 as compared to WT mice teeth (ratio 2.06). Larger pore size was observed consistently in D4 as compared to WT ($p=0.03$), in both sexes and both regions. Pore size was larger in the near DEJ region than mid-enamel region. ($p<0.001$) (Fig 5).

Some male:female differences were also seen across tooth regions. Near the DEJ, the enamel of male teeth was more porous in the proximal and occlusal regions than in the cervical region (P=0.097 for any difference among positions), whereas female teeth were more porous in the cervical and proximal regions than in the occlusal region (P=0.042 for any difference among positions in females; Figure 4b). The significance level is lower in male than female mice because of the difference in sample size (male: n=3, female: n=4). Near the DEJ, male mice tended to have higher pore counts in proximal and occlusal regions than cervical regions, whereas female mice tended to have higher pore counts in the proximal region than in the cervical and occlusal regions ($P > 0.15$).

Osteocalcin expression

Our data show severe defects in enamel porosity in D4 mice. However, in these mice, the osteocalcin promoter was expected to drive TGF-β2 overexpression only in odontoblasts; not in cells that formed enamel. To determine if the enamel defects were due to altered TGF-β2 expression by dentin or enamel producing cells, we confirmed the expression pattern of osteocalcin by *in situ* hybridization with a radiolabelled osteocalcin cRNA probe. *In situ* hybridization of the mouse molars showed osteocalcin expression in the dentin layer. However, since mouse molar enamel development is complete in 2 month old mice, ameloblasts were no longer present (Fig 6 A and B). Therefore we examined osteocalcin expression in the continuously erupting incisor, which contains all stages of dentin and enamel development in a single tooth. Osteocalcin mRNA also localized to odontoblast layer in the incisor, with no evidence of osteocalcin expression by the ameloblasts or in any other cells of the enamel organ (Fig. 6C and D) The expression patterns in both molars and incisors were similar in the WT and D4 mice.

Discussion

The TGF-β2 overexpressing transgenic mouse model examined in this study expresses an activated form of TGF-β2 linked to an osteocalcin promoter. Similar to our previous results (25), we did not find differences in nanohardnes between the transgenic and wildtype mouse dentin. However, in this study we did find significantly reduced dentin elastic modulus in the male TGF-β2 overexpressor mice, as compared to the other groups. The male TGF-β2 overexpressor mice exhibited an increased number of pores in the enamel, suggesting incomplete enamel formation. In this mouse model, the osteocalcin promoter drives TGF-β2 overexpression in dentin, but not enamel development. Therefore, these data indicate that the defects that are found in the enamel, result from changes in the response of the underlying dentin to TGF-β2 overexpression.

One explanation for the effects of TGF-β2 produced by odontoblasts, on enamel formation, is that the overexpressed TGF-β2 synthesized by the developing odontoblasts, directly contacts the epithelial cell layer prior to enamel matrix synthesis. An inhibition of pre-ameloblast proliferation or enhanced differentiation relative to exposure to higher levels of TGF-β is consistent with the known effects of TGF-β on epithelial cells (26).

However, it seems more likely that changes in the enamel of TGF-β2 overexpressing mice, result from altered dentin formation. Although the dentin layer in the transgenic mice appeared normal, nanomechanical testing showed a reduced elastic modulus in male D4 male mice. Increased enamel porosity was also found in this group of male D4 mice.

The phenotype of the TGF-β2 overexpressing mice is unlike those found in the transgenic mouse that overexpressed TGF-β1 linked to the dentin sialophosphoprotein (DSPP) promotor. The TGF-β1 overexpressor mice had a much more severe phenotype, with a highly disorganized odontoblast layer, and reduced dentin mineralization (27,28). However, in the

TGF-β1 mouse model, TGF-β overexpression was linked to the DSPP promotor, which is present in both the dental mesenchyme and epithelium. This, along with the requirement for a type III TGF-β receptor for efficient TGF-β2 activity (29) may account for the increased severity of the defects found in the TGF-β1 mouse model.

A surprising finding in this study were the differences between male and female mice. A possible explanation for the sex difference observed in the mouse teeth is that osteocalcin synthesis is greater in the odontoblasts of transgenic male mice, with resultant higher TGF-β2 synthesis in the male transgenic mice as compared to female transgenic mice. Studies in humans (30) and horses (31) have shown higher levels of osteocalcin in males as compared to females. The mechanism of sex-specific osteocalcin expression is not clear, and little information on sex-linked differences in tooth formation is available. These data suggest that sex differences should be considered when studying tooth formation.

The effect of overexpression of TGF-β2 by odontoblasts on enamel development, shown in this study emphasizes the importance of signaling by the dental mesenchyme on enamel formation. This study is the first to show sex-related differences in enamel structure, secondary to changes in dentin signaling. The presence of such porosities in enamel, would likely dramatically affect the resistance of this tissue to dental caries, since acids could more readily diffuse through the larger and more numerous pores. This suggests that genetic and environmentally-related differences in dentin signaling could alter enamel structure with a potential impact on dental health.

Acknowledgements

We gratefully acknowledge Diane Hu for her histological expertise and Grace Nonomura for preparation of the tissues. This work is supported by NIH/NIDCR Grant # P01DE09859.

References

1. Thesleff I, Vaahtokari A, Vainio S, Vaahtokari A, Jowett A. Molecular mechanisms of cell and tissue interactions during early tooth development. Anatomical Record 1996;245(2):151–61. [PubMed: 8769660]
2. Vaahtokari A, Vainio S, Thesleff I. Associations between transforming growth factor beta 1 RNA expression and epithelial-mesenchymal interactions during tooth morphogenesis. Development 1991;113(3):985–94. [PubMed: 1726565]
3. Kaartinen V, Voncken JW, Shuler C, Warburton D, Bu D, Heisterkamp N, et al. Abnormal lung development and cleft palate in mice lacking TGF-beta 3 indicates defects of epithelial-mesenchymal interaction. Nat Genet 1995;11(4):415–21. [PubMed: 7493022]
4. Loeys BL, Chen J, Neptune ER, Judge DP, Podowski M, Holm T, et al. A syndrome of altered cardiovascular, craniofacial, neurocognitive and skeletal development caused by mutations in TGFBR1 or TGFBR2. Nat Genet 2005;37(3):275–81. [PubMed: 15731757]
5. Proetzel G, Pawlowski SA, Wiles MV, Yin M, Boivin GP, Howles PN, et al. Transforming growth factor-beta 3 is required for secondary palate fusion. Nat Genet 1995;11(4):409–14. [PubMed: 7493021]
6. Bègue-Kirn C, Smith AJ, Loriot M, Kupferle C, Ruch JV, Lesot H. Comparative analysis of TGF beta s, BMPs, IGF1, msxs, fibronectin, osteonectin and bone sialoprotein gene expression during normal and in vitro-induced odontoblast differentiation. International Journal of Developmental Biology 1994;38(3):405–20. [PubMed: 7848824]
7. Heikinheimo K, Happonen RP, Miettinen PJ, Ritvos O. Transforming growth factor beta 2 in epithelial differentiation of developing teeth and odontogenic tumors. Journal of Clinical Investigation 1993;91(3):1019–27. [PubMed: 8450031]
8. He WX, Niu ZY, Zhao SL, Jin WL, Gao J, Smith AJ. TGF-beta activated Smad signalling leads to a Smad3-mediated down-regulation of DSPP in an odontoblast cell line. Arch Oral Biol 2004;49(11):911–8. [PubMed: 15353247]

9. Ruch JV, Lesot H, Baegue-Kirn C. Odontoblast differentiation. International Journal of Developmental Biology 1995;39(1):51–68. [PubMed: 7626422]
10. Thesleff I. Homeobox genes and growth factors in regulation of craniofacial and tooth morphogenesis. Acta Odontologica Scandinavica 1995;53(3):129–34. [PubMed: 7572087]
11. Xu X, Jeong L, Han J, Ito Y, Bringas P Jr, Chai Y. Developmental expression of Smad 1-7 suggests critical function of TGF-beta/BMP signaling in regulating epithelial-mesenchymal interaction during tooth morphogenesis. Int J Dev Biol 2003;47(1):31–9. [PubMed: 12653249]
12. Nakashima M, Nagasawa H, Yamada Y, Reddi AH. Regulatory role of transforming growth factor-beta, bone morphogenetic protein-2, and protein-4 on gene expression of extracellular matrix proteins and differentiation of dental pulp cells. Developmental Biology 1994;162(1):18–28. [PubMed: 8125185]
13. Liu H, Li W, Shi S, Habelitz S, Gao C, Denbesten P. MEPE is downregulated as dental pulp stem cells differentiate. Arch Oral Biol 2005;50(11):923–8. [PubMed: 16183369]
14. Toyono T, Nakashima M, Kuhara S, Akamine A. Expression of TGF-beta superfamily receptors in dental pulp. Journal of Dental Research 1997;76(9):1555–60. [PubMed: 9294489]
15. Huojia M, Muraoka N, Yoshizaki K, Fukumoto S, Nakashima M, Akamine A, et al. TGF-beta3 induces ectopic mineralization in fetal mouse dental pulp during tooth germ development. Dev Growth Differ 2005;47(3):141–52. [PubMed: 15839999]
16. Erlebacher A, Derynck R. Increased expression of TGF-beta 2 in osteoblasts results in an osteoporosis-like phenotype. Journal of Cell Biology 1996;132(12):195–210. [PubMed: 8567723]
17. Papagerakis P, Berdal A, Mesbah M, Peuchmaur M, Malaval L, Nydegger J, et al. Investigation of osteocalcin, osteonectin, and dentin sialophosphoprotein in developing human teeth. Bone 2002;30 (2):377–85. [PubMed: 11856645]
18. Bronckers AL, D'Souza RN, Butler WT, Lyaruu DM, van Dijk S, Gay S, et al. Dentin sialoprotein: biosynthesis and developmental appearance in rat tooth germs in comparison with amelogenins, osteocalcin and collagen type-I. Cell and Tissue Research 1993;272(2):237–47. [PubMed: 8513478]
19. Balooch M, Wu-Magidi IC, Balazs A, Lundkvist AS, Marshall SJ, Marshall GW, et al. Viscoelastic properties of demineralized human dentin measured in water with atomic force microscope (AFM)-based indentation. Journal of Biomedical Materials Research 1998;40(4):539–44. [PubMed: 9599029]
20. Habelitz S, Marshall SJ, Marshall GW Jr, Balooch M. Mechanical properties of human dental enamel on the nanometre scale. Arch Oral Biol 2001;46(2):173–83. [PubMed: 11163325]
21. Oliver WC, Pharr GM. An Improved Technique for Determining Hardness and Elastic-Modulus Using Load and Displacement Sensing Indentation Experiments. Journal of Materials Research 1992;7(6):1564–1583.
22. Oliver WC, Pharr GM. Measurement of hardness and elastic modulus by instrumented indentation: Advances in understanding and refinements to methodology. Journal of Materials Research 2004;19 (1):3–20.
23. Ferguson C, Alpern E, Miclau T, Helms JA. Does adult fracture repair recapitulate embryonic skeletal formation? Mech Dev 1999;87(12):57–66. [PubMed: 10495271]
24. Kang JS, Alliston T, Delston R, Derynck R. Repression of Runx2 function by TGF-beta through recruitment of class II histone deacetylases by Smad3. EMBO J 2005;24(14):2543–55. [PubMed: 15990875]
25. DenBesten PK, Machule D, Gallagher R, Marshall GW Jr, Mathews C, Filvaroff E. The effect of TGF-beta 2 on dentin apposition and hardness in transgenic mice. Adv Dent Res 2001;15:39–41. [PubMed: 12640737]
26. Derynck R. TGF-beta-receptor-mediated signaling. Trends in Biochemical Sciences 1994;19(12): 548–53. [PubMed: 7846768]
27. Thyagarajan T, Sreenath T, Cho A, Wright JT, Kulkarni AB. Reduced expression of dentin sialophosphoprotein is associated with dysplastic dentin in mice overexpressing transforming growth factor-beta 1 in teeth. J Biol Chem 2001;276(14):11016–20. [PubMed: 11116156]
28. Haruyama N, Thyagarajan T, Skobe Z, Wright JT, Septier D, Sreenath TL, et al. Overexpression of transforming growth factor-beta1 in teeth results in detachment of ameloblasts and enamel defects. Eur J Oral Sci 2006;114(Suppl 1):30–4. [PubMed: 16674659]

29. Derynck R, Feng XH. TGF-beta receptor signaling. Biochim Biophys Acta 1997;1333(2):F105–50. [PubMed: 9395284]

30. Fares JE, Choucair M, Nabulsi M, Salamoun M, Shahine CH, Fuleihan Gel H. Effect of gender, puberty, and vitamin D status on biochemical markers of bone remodedeling. Bone 2003;33(2):242–7. [PubMed: 14499358]

31. Carstanjen B, Amory H, Sulon J, Hars O, Remy B, Langlois P, et al. Serum osteocalcin and CTX-MMP concentration in young exercising thoroughbred racehorses. J Vet Med A Physiol Pathol Clin Med 2005;52(3):114–20. [PubMed: 15836441]

Abbreviations

TGF-β
: transforming growth factor-β

SEM
: scanning electron microscopy

AFM
: atomic force microscopy

BMP
: bone morphogenetic protein

DAPI
: 4’, 6-diamidino-2-phenyindole

DSPP
: dentin sialophosphoprotein

WT
: wildtype mice

D4
: TGF-β overexpressor transgenic mice

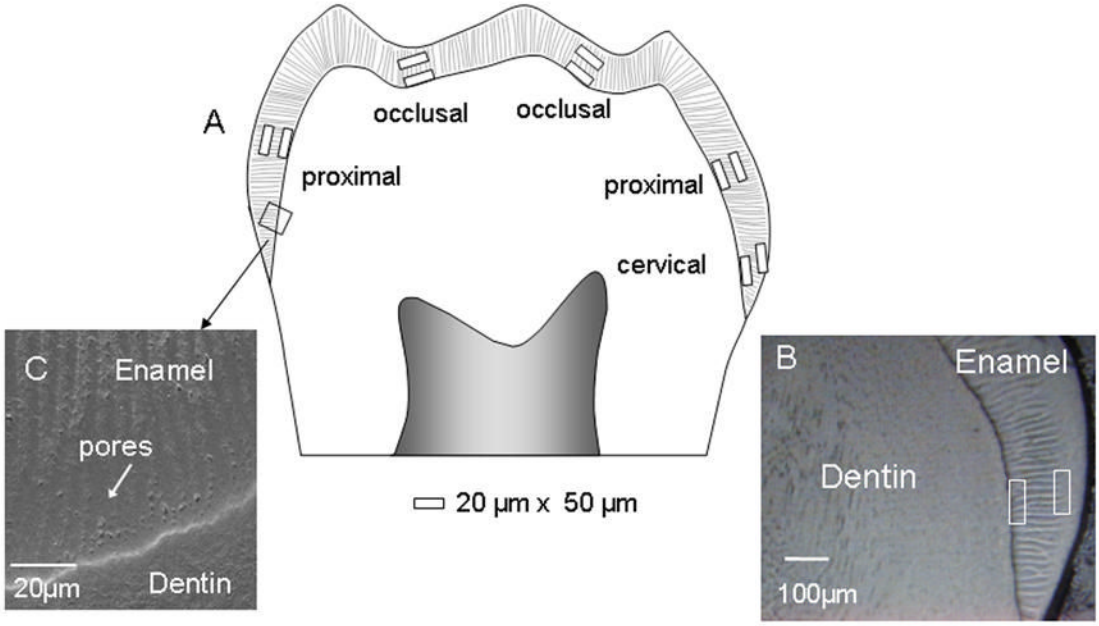

Figure 1.
A: Schematic drawing of examined area on sagittal section of first molar. B: optical microscopic image (male WT) squares show the examined area in A. C: SEM (backscattered) showing porous structure of enamel.

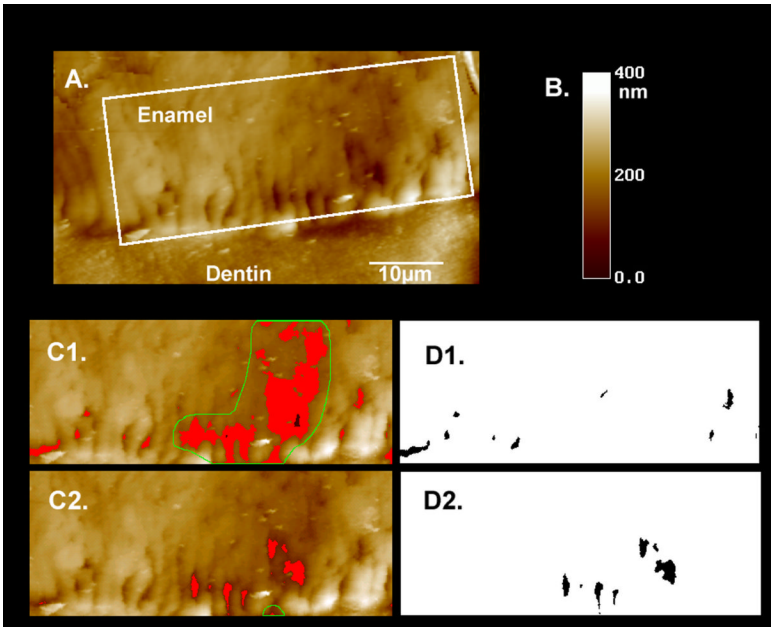

Figure 2.

These panels show an example of how the AFM images were processed with Scion Image™. A: Topographic image captured by AFM. A 20×50 μm area (shown as white outlined box) along the DEJ was selected. B) The z axis value is shown in the chromatic scales to the right of the image, with darker colors showing lower topography, representing pores in the enamel. C) The Scion image system was used to identify pores by color, with pores defined as small dark spots. When capturing the images of pores in the lighter elevated regions, larger concave areas were falsely identified (green outlined area). These areas were manually deleted and a second image (C2) was made of the pores in the darker concave regions. These two images were transferred to a black scale (binarized) and the total number and size (area) of the pores were counted and recorded.

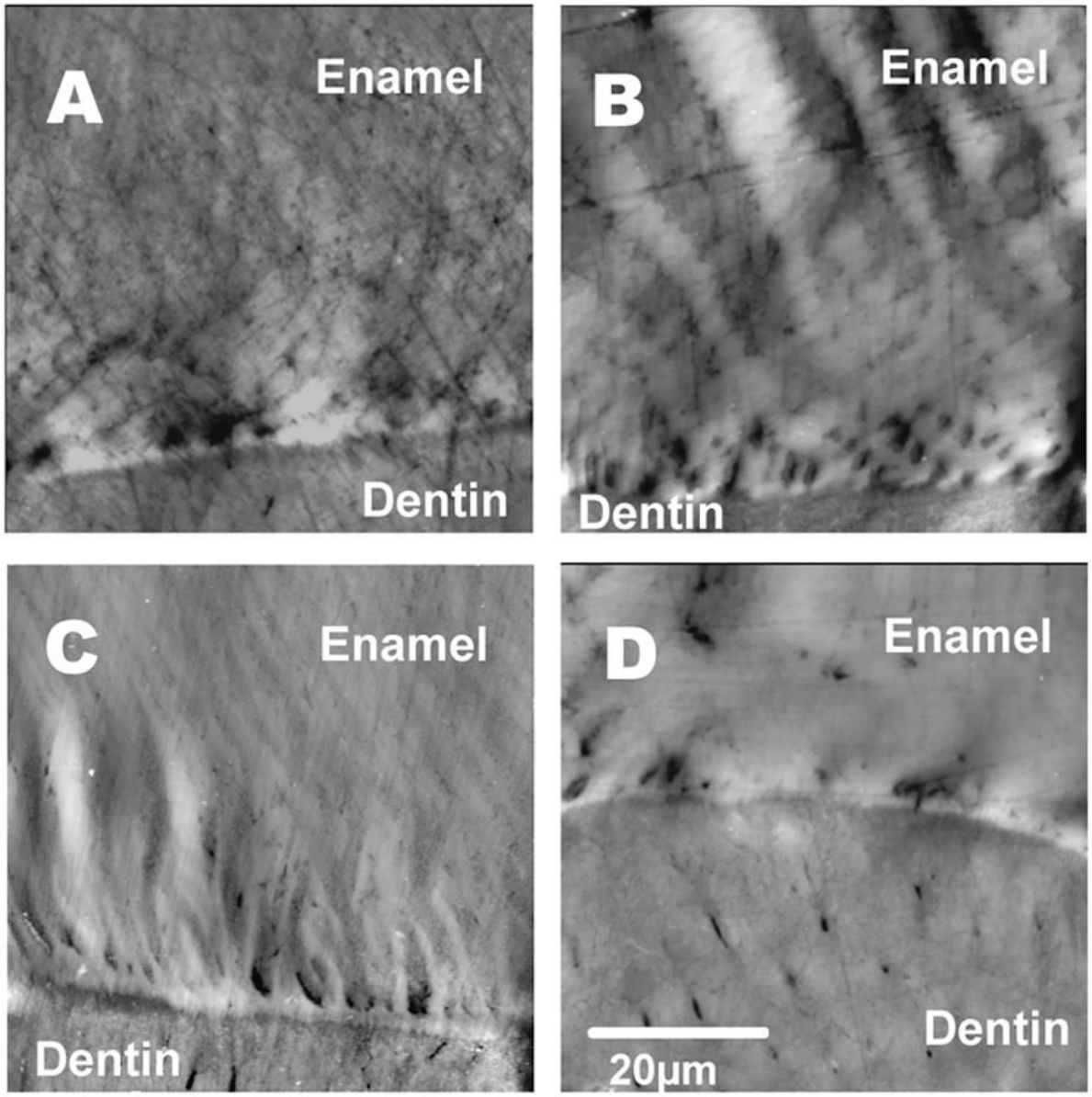

Figure 3.
AFM topographic images of the occlusal area of enamel near the DEJ. A: WT male, B: D4 male, C: WT female, D: D4 female. More pores were apparent in the D4 male.

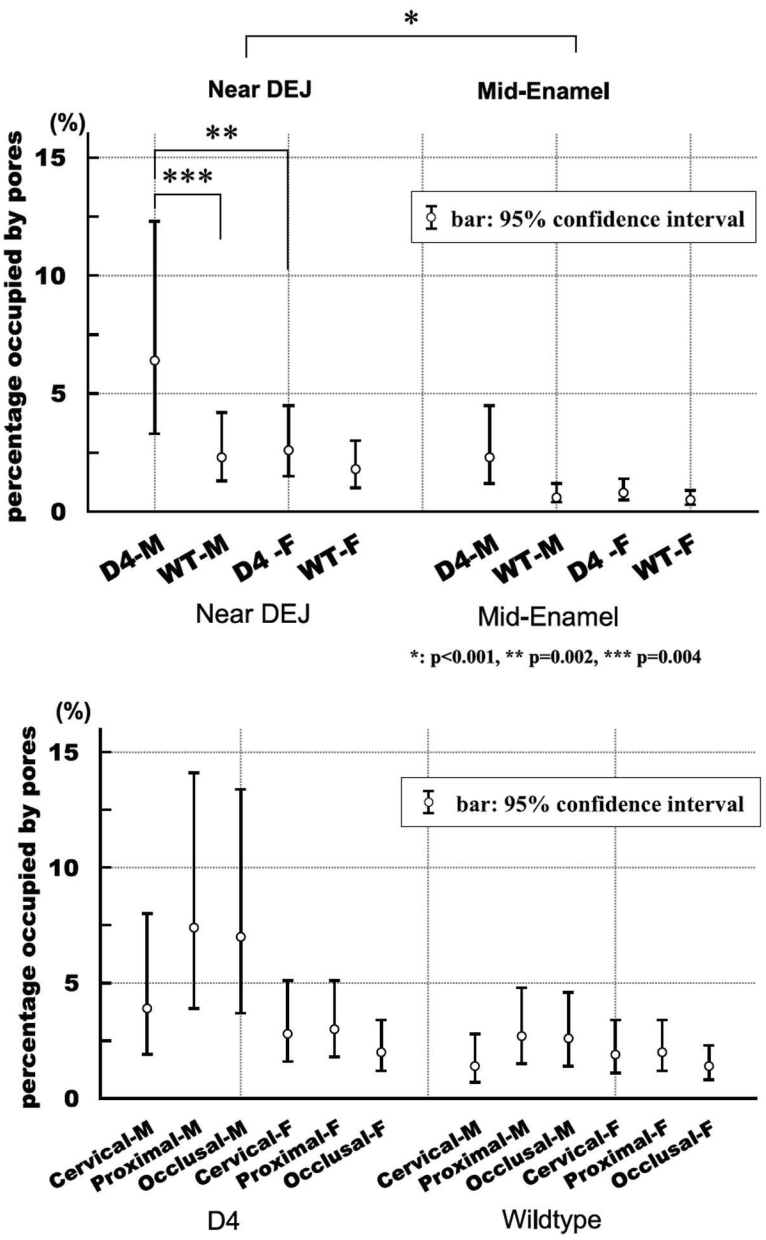

Figure 4.

a. Percentage of 1000 μm^2 field occupied by pores, by tissue type, mouse type, and sex. Plotted are means (95% confidence interval), per tissue type, over 3 male mice at 8 positions; 4 female mice at 8 positions. Pore areas in enamel are greatest in D4 male mice, in which pores occupied 3.3-fold more area near the DEJ than in mid-enamel ($p<0.001$).

b. Enamel near the DEJ: Percentage of 1000 μm^2 field occupied by pores, by mouse type, tissue location, and mouse sex. Plotted are means (95% confidence interval), per tissue type, over 3 male mice at 2 cervical, 3 proximal, and 3 occlusal positions; and 4 female mice at 2 cervical, 3 proximal, and 3 occlusal positions. Male teeth are more porous in the proximal and occlusal regions than in the cervical region, whereas female teeth are more porous in the cervical and proximal regions than in the occlusal region (tests of variation by position: male, $P=0.097$; female, $P=0.042$).

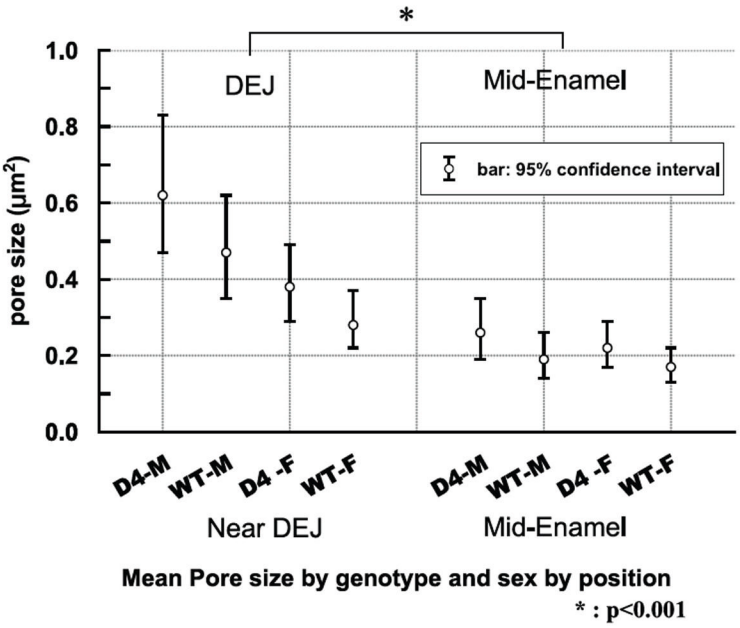

Figure 5.

Pore size (μm^2), by tissue type, mouse type, and sex. Plotted are means (95% confidence interval), per tissue type, over 3 male mice at 8 positions; 4 female mice at 8 positions. Pore size is larger in D4 than WT, after controlling for tissue type and sex (P=0.03). Pore size is larger in enamel near the DEJ than in the mid-enamel region (P<0.001).

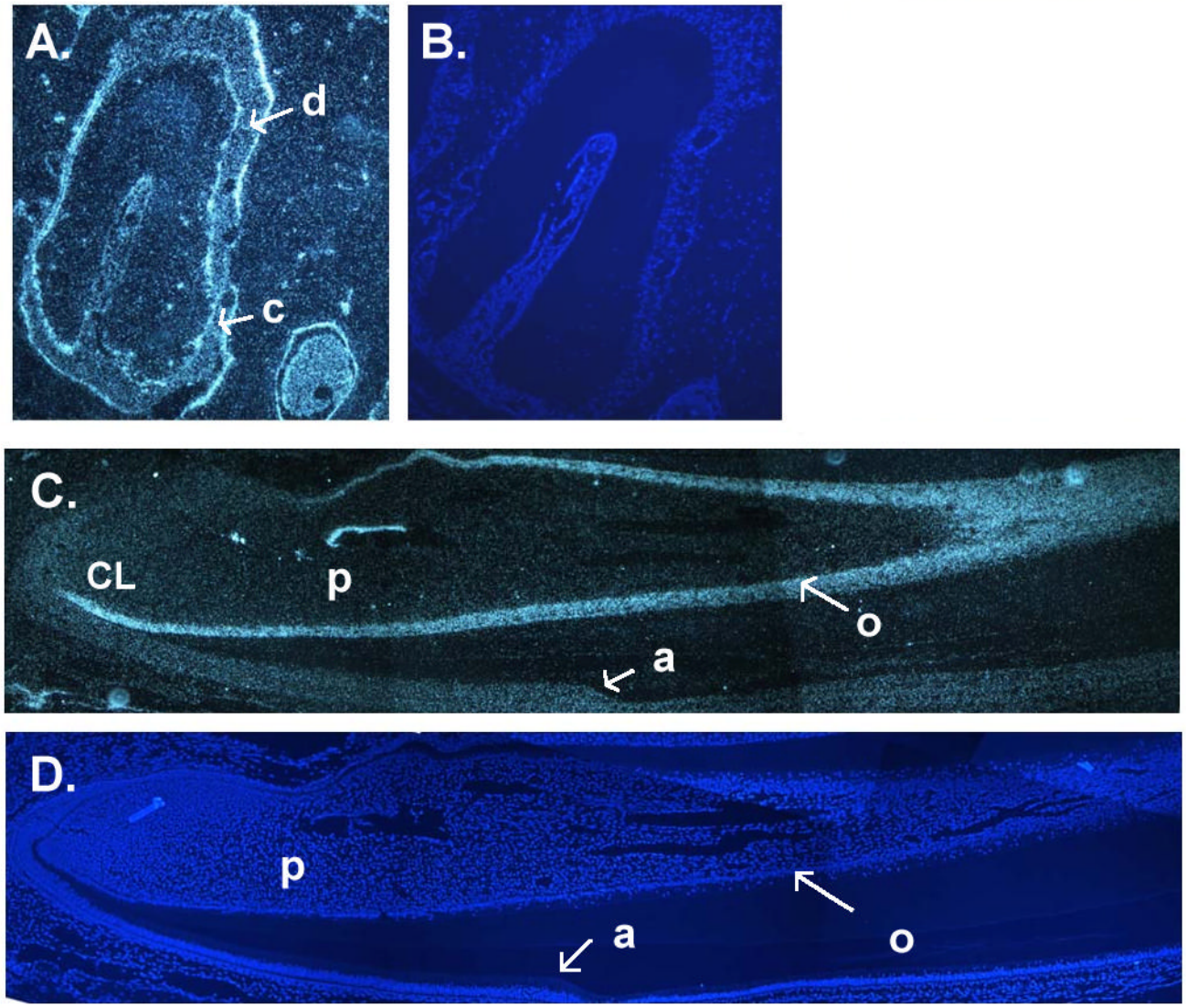

Figure 6.

In situ hybridization of the TGF-β mouse teeth. Molars showed osteocalcin expression in the dentin (d) and cementum (c) layers (A). Antisense control shows no staining (B). However, since mouse molar enamel development is complete in 2 month old mice, ameloblasts (a) were no longer present. Osteocalcin *in situ* hybridization (C) and control (D) of incisors show the cervical loop (CL) area where enamel formation is initiated up to the enamel maturation stage. At all stages of enamel formation only the dentin is positive for osteocalcin mRNA, indicating that alterations in the enamel of the TGF-β mice are secondary to TGF-β_2 overexpression by the odontoblasts (o), pulp (p).

Table 1

Dentin Mechanical Properties

Group	Elastic modulus (GPa) Mean (95% CI)	Hardness (GPa) Mean (95% CI)
Female WT	17.5 (15.0 – 19.9)*	0.71 (0.57 – 0.85)
Female D4	16.3 (14.2 – 18.5)	0.73 (0.60 – 0.86)
Male WT	15.1 (13.0 – 17.2)	0.62 (0.50 – 0.75)
Male D4	9.6 (7.5 – 11.8)	0.55 (0.42 – 0.67)